



1 **Modernizing the open-source community Noah-MP land surface model (version 5.0) with**
2 **enhanced modularity, interoperability, and applicability**

3

4 Cenlin He¹, Prasanth Valayamkunnath^{1,5}, Michael Barlage², Fei Chen¹, David Gochis¹, Ryan
5 Cabell¹, Tim Schneider¹, Roy Rasmussen¹, Guo-Yue Niu³, Zong-Liang Yang⁴, Dev Niyogi⁴,
6 Michael Ek¹

7

8 ¹National Center for Atmospheric Research (NCAR), Boulder, Colorado, USA

9 ²NOAA Environmental Modeling Center (EMC), College Park, Maryland, USA

10 ³University of Arizona, Tucson, Arizona, USA

11 ⁴University of Texas Austin, Austin, Texas, USA

12 ⁵Indian Institute of Science Education and Research Thiruvananthapuram, India

13

14

15 *Correspondence to:* Cenlin He (cenlinhe@ucar.edu)

16

17

18

19 **Abstract**

20

21 The widely-used open-source community Noah-MP land surface model (LSM) is designed for
22 applications ranging from uncoupled land-surface and ecohydrological process studies to coupled
23 numerical weather prediction and decadal global/regional climate simulations. It has been used in
24 many coupled community weather/climate/hydrology models. In this study, we
25 modernize/refactor the Noah-MP LSM by adopting modern Fortran code and data structures and
26 standards, which substantially enhances the model modularity, interoperability, and applicability.
27 The modernized Noah-MP is released as the version 5.0 (v5.0), which has five key features: (1)
28 enhanced modularization and interoperability by re-organizing model physics into individual
29 process-level Fortran module files, (2) enhanced data structure with new hierarchical data types
30 and optimized variable declaration and initialization structures, (3) enhanced code structure and
31 calling workflow by leveraging the new data structure and modularization, (4) enhanced
32 (descriptive and self-explanatory) model variable naming standard, and (5) enhanced driver and
33 interface structures to couple with host weather/climate/hydrology models. In addition, we create
34 a comprehensive technical documentation of the Noah-MP v5.0 and a set of model benchmark and
35 reference datasets. The Noah-MP v5.0 will be coupled to various weather/climate/hydrology
36 models in the future. Overall, the modernized Noah-MP will allow a more efficient and convenient
37 process for future model developments and applications.

38

39

40



41 **1. Introduction**

42

43 Land surface models (LSMs) are useful modeling tools to resolve terrestrial responses to and
44 interactions with the atmosphere, ocean, glacier, and sea ice in the earth system. Traditionally,
45 LSMs were thought to mainly provide lower boundary conditions to the coupled atmospheric
46 models. However, modern LSMs have been increasingly employed as an indispensable component
47 in the climate and weather systems to offer biogeophysical and biogeochemical insight for
48 understanding and quantifying the impact and evolution of climate, weather, and the integrated
49 earth environment (Blyth et al., 2021). LSMs have been widely applied to tackle many important
50 societally relevant challenges, such as drought, flood, heat wave, water availability, agriculture,
51 food security, wildfires, deforestation, and urbanization (Bonan and Doney, 2018).

52

53 Among many LSMs that have been developed in the past few decades, the open-source community
54 Noah with Multi-parameterization Options (Noah-MP; Niu et al., 2011; Yang et al., 2011) is one
55 of the most widely-used state-of-the-art LSMs. The article describing the Noah-MP model by Niu
56 et al (2011) is *de facto* the most cited LSM paper in the last 10 years, highlighting its worldwide
57 popular usage in the international science community. Compared to its predecessor, the Noah LSM
58 (Chen et al., 1996, 1997; Chen and Dudhia, 2001; Ek et al., 2003), Noah-MP significantly
59 improves known Noah limitations by employing enhanced treatments of vegetation canopy,
60 snowpack, soil processes, groundwater, and their complex interactions as well as additional
61 capabilities for critical land processes (e.g., crop, irrigation, tile drainage, groundwater, urban,
62 carbon and nitrogen cycles). Another unique feature of Noah-MP is the inclusion of multiple
63 physics options for different land processes, which allows the multi-physics model ensemble
64 experiments for uncertainty assessment and testing competing hypotheses (Zhang et al., 2016; J.
65 Li et al., 2020).

66

67 Noah-MP can be applied to various spatial scales spanning from point scale locally to ~100-km
68 resolution globally, and temporal scales spanning from sub-daily to decadal time scales. Since its
69 original development, Noah-MP has been used in many important applications, including
70 numerical weather prediction (Suzuki and Zupanski, 2018; Ju et al., 2022), high-resolution climate
71 modeling (Gao et al., 2017; Liu et al., 2017; Rasmussen et al., 2023), land data assimilation (Xu
72 et al., 2021; Nie et al., 2022), drought (Arsenault et al., 2020; Niu et al., 2020; Wu et al., 2021;
73 Abolafia-Rosenzweig et al., 2023a), wildfire (Kumar et al., 2021; Abolafia-Rosenzweig et al.,
74 2022a, 2023b), snowpack evolution (Wrzesien et al., 2015; He et al., 2019; Jiang et al., 2020),
75 hydrology and water resources (Cai et al., 2014; Liang et al., 2019; X. Zhang et al., 2022a; Hazra
76 et al., 2023), crop and agricultural management (Liu et al., 2016; Ingwersen et al., 2018; Warrach-
77 Sagi et al., 2022; Valayamkunnath et al., 2022; Zhang et al., 2020, 2023), urbanization and heat
78 island (Xu et al., 2018; Salamanca et al., 2018; Patel et al., 2022), biogeochemical cycle (Cai et
79 al., 2016; Brunsell et al., 2021), wind erosion (Jiang et al., 2021), wetland (Z. Zhang et al., 2022),
80 groundwater (Barlage et al., 2015, 2021; Li et al., 2022), and landslide hazard (Zhuo et al., 2019).



81

82 Currently, Noah-MP has been implemented into many community research and operational
83 weather/climate/hydrology models, including the Weather Research and Forecasting model
84 (WRF), the Model for Prediction Across Scales (MPAS), the NOAA operational National Water
85 Model (NWM), the NOAA Unified Forecast System (UFS), the NASA Land Information System
86 (LIS), and the NCAR High-Resolution Land Data Assimilation System (HRLDAS).

87

88 Despite its popular usage in the international research and application communities, the Noah-MP
89 core code engine was designed 12 years ago and is outdated, and does not take advantage of
90 modern Fortran language architecture. It has a single lengthy (>12,000 lines) Fortran source file
91 lumping together all model physics with complex code and data structures using inconsistent
92 format and does not follow the modern Fortran code standard. This makes the Noah-MP model
93 code difficult for users and developers to read, modify, and test as well as to implement and apply
94 it to other community models. Furthermore, a lengthy code is error prone and challenging to debug.
95 These issues limit the further development and application of Noah-MP.

96

97 Therefore, this study is motivated to modernize (refactor) the entire Noah-MP model by adopting
98 modern Fortran code and data structures and standards, which substantially enhances the model
99 modularity, interoperability, and applicability. The base code used for refactoring is the Noah-MP
100 version 4.5 (released in December 2022; [https://github.com/NCAR/noahmp/tree/release-v4.5-](https://github.com/NCAR/noahmp/tree/release-v4.5-WRF)
101 [WRF](https://github.com/NCAR/noahmp/tree/release-v4.5-WRF)), and the refactoring effort does not change model physics. We release the
102 modernized/refactored Noah-MP as version 5.0 (v5.0; <https://github.com/NCAR/noahmp>), which
103 includes five key features: (1) enhanced modularization and interoperability by re-organizing
104 model physics into individual process-level Fortran module files, (2) enhanced data structure with
105 new hierarchical data types and optimized variable declaration and initialization structures, (3)
106 enhanced code structure and subroutine calling workflow by leveraging the new data structure and
107 modularization and refining code to be more concise, (4) enhanced (descriptive and self-
108 explanatory) model variable naming standard, and (5) enhanced driver and interface code
109 structures to couple with host weather/climate/hydrology models. In addition, we have created a
110 comprehensive technical documentation (He et al., 2023) to describe model physics and details of
111 the refactored Noah-MP and a set of model benchmark and reference datasets for future
112 comparison and assessment. Overall, the modernized open-source community Noah-MP model
113 (version 5.0) will allow a more efficient and convenient process for future model developments
114 and applications. The framework and practice in the course of refactoring the entire Noah-MP code
115 is also applicable to other LSMs and ESMs.

116

117 This paper reports the key features of the modernized Noah-MP v5.0 and is organized as follows.
118 Section 2 briefly summarizes the Noah-MP model physics with several updates since its original
119 development. Sections 3–7, respectively, introduce the key features of the modernized Noah-MP
120 in terms of enhanced model modularization, data type, code structure, variable naming, and



121 coupling structure with host models. Section 8 describes the model benchmarking and reference
122 datasets. Section 9 provides the release information of model code and technical documentation.
123 Section 10 concludes the paper with future model development plans.

124

125 **2. Noah-MP version 5.0 model physics**

126

127 **2.1 Noah-MP description**

128

129 Noah-MP (Niu et al., 2011) was originally developed based on the Noah LSM (Chen et al., 1996,
130 1997; Chen and Dudhia, 2001; Ek et al., 2003) to augment its modeling capabilities with enhanced
131 physical representations and treatments of dynamic vegetation, canopy interception and radiative
132 transfer processes, multi-layer snowpack physics, and soil and hydrological processes. The history
133 of model development and evolution has been described in the technical documentation (He et al.,
134 2023). Noah-MP is designed to simulate land surface and subsurface energy and water processes
135 in both uncoupled and coupled modes with atmospheric or hydrological models at sub-daily time
136 scale and high spatial resolution (even for point scale). This further allows the use of Noah-MP in
137 different hydrological, weather, and climate models for applications in a wide range of spatial and
138 temporal scales with proper integration in time and space.

139

140 Noah-MP divides its land grid into two sub-grid tiles, namely vegetated and non-vegetated grounds,
141 based on vegetation cover fraction. The biogeophysical and biogeochemical processes are treated
142 separately for the vegetated and bare grounds. Noah-MP adopts a “big-leaf” canopy treatment
143 characterized by canopy properties dependent on vegetation types. Noah-MP accounts for a
144 multiple-layer snowpack, where snow ice and liquid water content, density, depth, and temperature
145 are simulated dynamically. Noah-MP also includes multi-layer soil thermal and hydrological
146 processes with dynamically evolving soil temperature and water content. The vegetation, snow,
147 and soil components in Noah-MP are closely coupled and interacted with each other via complex
148 energy, water, and biochemical processes. Their detailed physical formulations and
149 parameterizations in Noah-MP v5.0 are described in the technical documentation (He et al., 2023).
150 Below, we briefly summarize the energy, water, and biochemical processes in Noah-MP v5.0.

151

152 **2.2 Noah-MP energy processes**

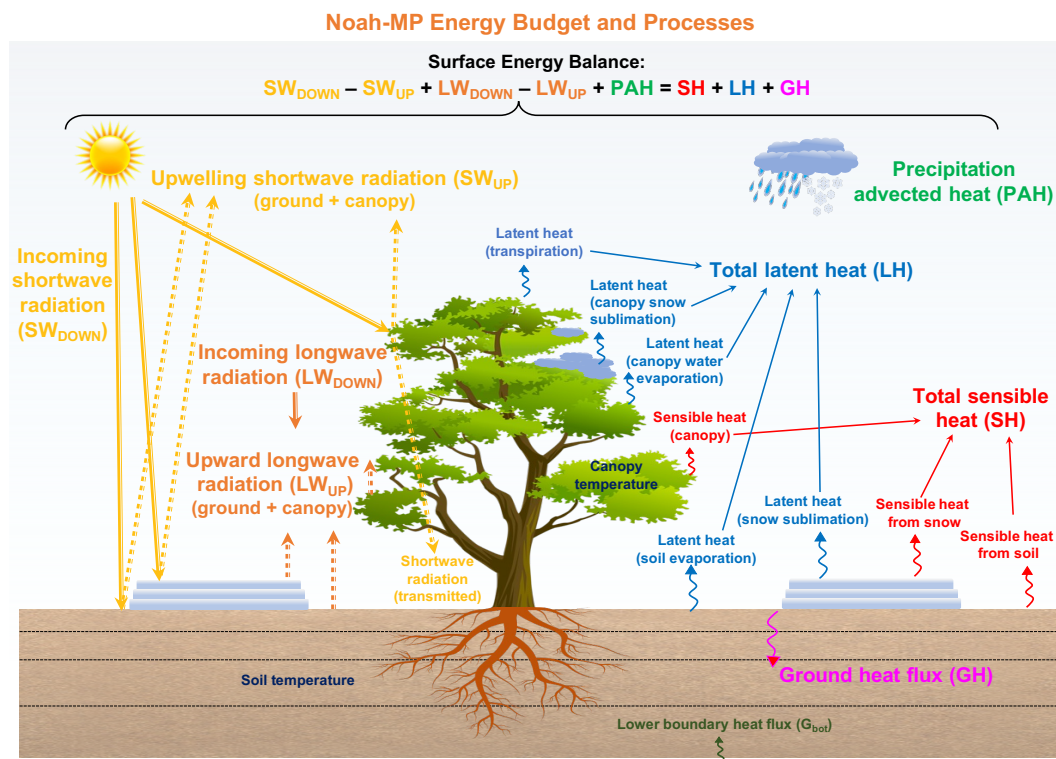
153

154 Noah-MP resolves energy budgets and processes separately for vegetated and non-vegetated
155 ground portions of each grid (Niu et al., 2011). The vegetation cover fraction, either from
156 observational inputs or model calculations based on leaf area index (LAI) inputs or predicted by
157 the dynamic vegetation module, is used to separate vegetated and bare grounds. The grid-mean
158 energy states and fluxes are calculated as an average of vegetated and bare ground values weighted
159 by vegetation cover fraction. For surface radiative processes driven by incoming shortwave and
160 longwave radiation (atmospheric forcing), Noah-MP simulates the radiative absorption and



161 scattering by the canopy and ground (soil/snow) as well as the longwave emissions by the canopy
162 and ground (soil/snow). The net absorbed total (shortwave and longwave) radiative flux is
163 balanced by precipitation advected heat flux, total surface sensible and latent heat fluxes, and
164 ground heat flux. The precipitation advected heat flux represents the heat flux advected from
165 precipitation (rain/snow) to canopy/ground due to the temperature difference between precipitation
166 (surface air) and canopy/ground. The total surface sensible heat includes the sensible heat from
167 canopy, snowpack, and soil surfaces. The total surface latent heat includes the latent heat from
168 snowpack sublimation, soil evaporation, canopy snow sublimation, canopy water evaporation, and
169 plant transpiration. The ground heat flux is the heat flux leaving the ground surface to drive
170 subsurface snow/soil phase change and/or temperature changes.

171
172 To model the aforementioned surface energy flux components, Noah-MP dynamically calculates
173 a number of key land surface properties, include ground snow cover fraction, surface roughness,
174 canopy and ground thermal properties, snow and soil albedo, surface emissivity, and canopy
175 radiative transfer. Many of these property and process calculations have multiple physics options
176 (see Sect. 2.6). Based on the canopy and ground energy balance, Noah-MP further solves the
177 temperature and phase change for canopy, snowpack, and soil. Figure 1 summarizes the key energy
178 processes and budget components as well as the energy balance equation in Noah-MP v5.0. Note
179 that the energy processes at glacier grids are treated similarly to those at 100% bare (non-vegetated)
180 ground grids except that the soil is replaced by glacier ice with ice-specific properties.
181



182

183 **Figure 1.** Schematic diagram of energy budget and processes represented in Noah-MP version 5.0.

184

185

186

2.3 Noah-MP water processes

187

188

189

190

191

192

193

194

195

196

197

198

199

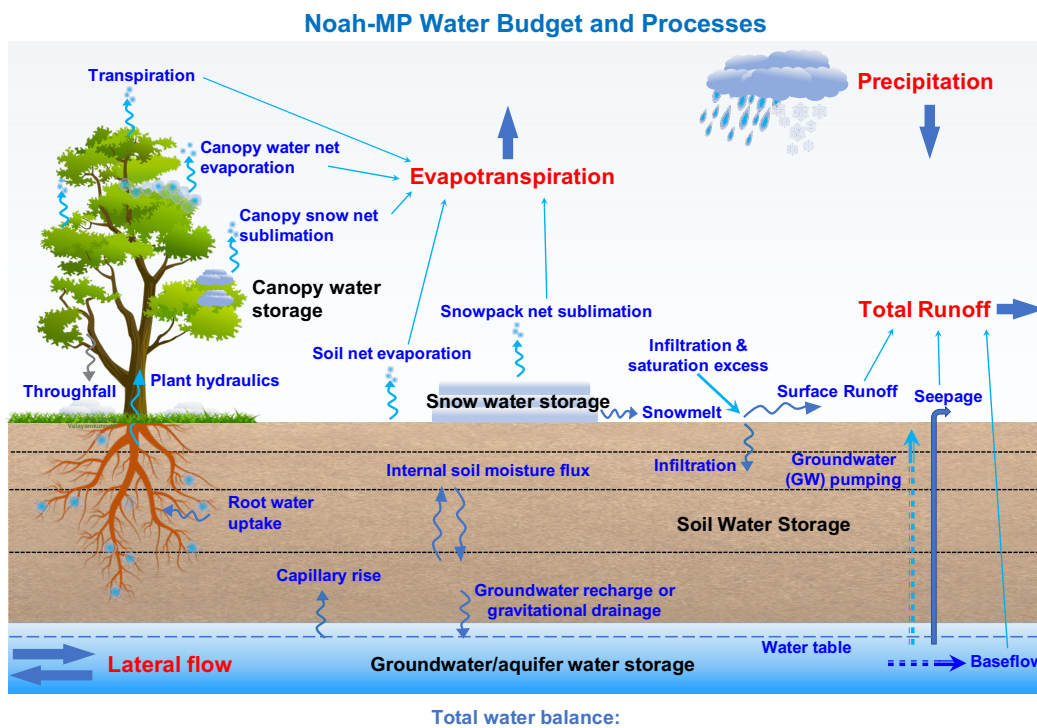
200

201

Noah-MP accounts for five major water budget components, including precipitation, evapotranspiration (ET), total runoff, net lateral flow, and total water storage change intercepted by the canopy and in snow, soil, and aquifer. For precipitation, Noah-MP has several temperature-based rainfall-snowfall partitioning parameterizations or can use the partitioning from atmospheric models directly (see Sect. 2.6). Noah-MP simulates canopy interception and throughfall of rain and snow, where the intercepted rain and snow on the canopy can go through unloading/dripping, frost, sublimation, melting, and freezing processes. Net evaporation loss from the canopy-intercepted liquid water (evaporation minus dew), net sublimation from the canopy-intercepted snow (sublimation minus frost), transpiration (via plant hydraulics), net soil surface evaporation, and net snowpack sublimation together contribute to the total surface ET. Noah-MP dynamically simulates multi-layer snowpack water storage (ice and liquid water) changes driven by snowfall/rainfall, frost, sublimation, freezing, and melting. The snowmelt water out of snowpack together with rainfall at the soil surface are further partitioned into surface runoff and infiltration based on multiple runoff and infiltration physics options (see Sect. 2.6). Soil moisture and



202 unsaturated water flow across soil layers are simulated using the one-dimensional Richards
 203 equation. Two optional groundwater schemes, one without 2-D lateral flow (Niu et al., 2007) and
 204 one with 2-D lateral flow (Fan et al., 2007; Miguez-Macho et al. 2007), are available in Noah-MP
 205 to simulate groundwater dynamics, including groundwater recharge, water table change, baseflow,
 206 seepage, and/or lateral flow. Noah-MP also includes dynamic irrigation and tile drainage processes
 207 for agricultural management applications (Valayamkunnath et al., 2021, 2022). Figure 2
 208 summarizes the key water processes and budget components as well as the water balance equation
 209 in Noah-MP v5.0. Note that the water processes at glacier grids are treated similarly to those at
 210 100% bare ground grids except that all the soil and subsurface hydrological processes are removed
 211 and replaced by glacier ice (He et al., 2023).
 212



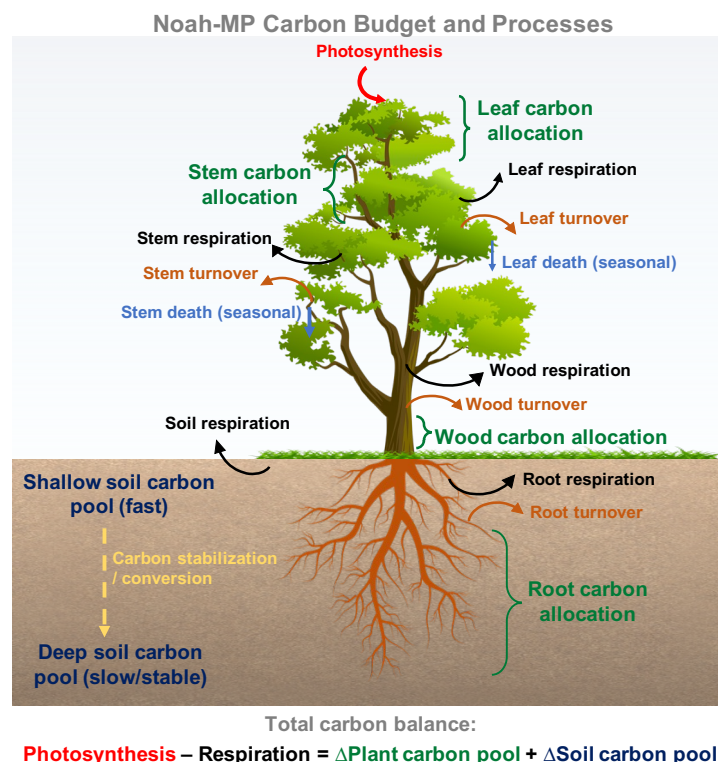
213 **Figure 2.** Schematic diagram of water budget and processes represented in Noah-MP version 5.0.
 214
 215

216
 217 **2.4 Noah-MP biochemical processes**

218
 219 Currently, the community version of Noah-MP only accounts for carbon processes for biochemical
 220 cycles, while nitrogen dynamics and soil carbon dynamics have been developed in non-community
 221 Noah-MP versions managed by individual research groups (e.g., Cai et al., 2016; X. Zhang et al.,



222 2022b). We will synthesize and integrate individual Noah-MP updates into the community version
 223 in the future (see Sect. 2.5 for more discussions). Noah-MP simulates carbon processes for both
 224 natural/generic vegetation (Niu et al., 2011) and explicit agricultural crops (Liu et al., 2016). The
 225 carbon processes related to vegetation growth dynamics include (1) carbon assimilation from
 226 photosynthesis by shaded and sunlit leaves, (2) carbon allocation to different parts of vegetation
 227 (leaf, stem, wood and root) and soil carbon pools (fast and slow carbon), (3) carbon loss due to
 228 respiration of different vegetation and soil carbon pools, (4) carbon transfer between vegetation
 229 and fast soil carbon pools through vegetation (leaf, stem, wood and root) turnover and seasonal
 230 death of leaf and stem, and (5) soil carbon pool conversion through soil carbon stabilization. The
 231 total carbon flux to the atmosphere and net primary productivity are computed based on the
 232 aforementioned carbon processes. Figure 3 summarizes the key carbon processes and budget
 233 components as well as the carbon balance equation in Noah-MP v5.0. Note that the carbon
 234 processes for crop growth are treated similarly to those of natural vegetation, except that the wood
 235 component of plants is removed and the grain component of crops is added with additional carbon
 236 conversion from leaf, stem, and root to grain depending on crop growing stages.
 237



238

239

240

241

Figure 3. Schematic diagram of carbon budget and processes represented in Noah-MP version 5.0.



242 **2.5 Noah-MP physics updates since original development**

243

244 Since the release of the original Noah-MP in year 2011 (Niu et al., 2011), there are several
245 important updates in Noah-MP physics. Some of the updates have been included in the community
246 version of Noah-MP v5.0, while some are only available in the non-community versions managed
247 by individual research groups. We will make efforts to synthesize and integrate individual Noah-
248 MP updates into the community version in the future by working with those developer teams. Here,
249 to the best of our knowledge, we briefly list the major Noah-MP physics updates from the
250 community in the past decade.

251

252 The new/enhanced physics included in the community Noah-MP version 5.0 since 2011 are: (1)
253 the Miguez-Macho-Fan (MMF) groundwater scheme (Barlage et al., 2015); (2) three additional
254 runoff schemes: the Variable infiltration capacity (VIC), dynamic VIC, and Xinanjiang schemes
255 (McDaniel et al., 2020); (3) tile drainage schemes (Valayamkunnath et al., 2022); (4) dynamic
256 irrigation schemes (sprinkler, micro, and flooding irrigation) (Valayamkunnath et al., 2021); (5) a
257 dynamic crop growth model for corn and soybean (Liu et al., 2016) with enhanced C3 and C4 crop
258 parameters (Zhang et al., 2020); (6) coupling with urban canopy models (Xu et al., 2018;
259 Salamanca et al., 2018) with local climate zone modeling capabilities (Zonato et al., 2021); (7)
260 enhanced snow cover, snow compaction, and wind-canopy absorption parameters (He et al., 2021);
261 (8) a wet-bulb temperature-based snow-rain partitioning scheme (Wang et al., 2019).

262

263 The new/enhanced physics currently not included in the community Noah-MP version 5.0 since
264 2011 are: (1) nitrogen dynamics (Cai et al., 2016); (2) big-tree plant hydraulics (Li et al., 2021);
265 (3) dynamic root optimization (Wang et al. 2018) with an explicit representation of plant water
266 storage (Niu et al., 2020); (4) additional snow cover parameterizations (Jiang et al., 2020); (5)
267 coupling with a wind erosion model (Jiang et al., 2021); (6) a wetland representation and dynamics
268 (Z. Zhang et al., 2022); (7) a unified turbulence parameterization throughout the canopy and
269 roughness sublayer (Abolafia-Rosenzweig et al., 2021); (8) enhanced snow albedo representations
270 (Abolafia-Rosenzweig et al., 2022b); (9) coupling with a snow radiative transfer (SNICAR) model
271 (Wang et al., 2020, 2022); (10) an organic soil layer representation at forest floors (Chen et al.,
272 2016) and a microbial-explicit soil organic carbon decomposition model (MESDM; X. Zhang et
273 al., 2022b); (11) coupling with atmospheric dry deposition of air pollutant (Chang et al., 2022);
274 (12) enhanced permafrost soil representations (X. Li et al., 2020); (13) spring wheat crop dynamics
275 (Zhang et al., 2023); (14) new treatment of thermal roughness length (Chen and Zhang 2009); (15)
276 the Gecros crop model (Ingwersen et al., 2018; Warrach-Sagi et al., 2022); (16) a 1-D dual-
277 permeability flow model (based on the mixed-form Richards' equation) representing preferential
278 flow through variably-saturated soil with surface ponding being developed in the University of
279 Arizona.

280

281 **2.6 Noah-MP multi-physics options**



282

283 One unique feature and advantage of Noah-MP is the inclusion of multiple physics options for
 284 different land processes for testing competing hypotheses (i.e., options) and multi-model ensemble
 285 simulations. Table 1 summarizes all the available physics options in the community Noah-MP
 286 v5.0. In particular, compared to previous Noah-MP versions, we have separated the runoff options
 287 for surface and subsurface runoff processes, and added a new physics option for snow thermal
 288 conductivity calculations, which were originally hard-coded without the namelist control
 289 capability. More detailed descriptions of each physics option are provided in the technical
 290 documentation (He et al., 2023).

291

292

Table 1. List of Noah-MP version 5.0 multi-physics options

Noah-MP Physics	Option	Notes (* indicates the default option)
OptDynamicVeg options for dynamic (prognostic) vegetation	1	off (use table LeafAreaIndex; use VegFrac = VegFracGreen from input) (Niu et al., 2011; Yang et al., 2011)
	2	on (together with OptStomataResistance = 1) (Dickinson et al., 1998; Niu and Yang, 2003)
	3	off (use table LeafAreaIndex; calculate VegFrac)
	4*	off (use table LeafAreaIndex; use maximum vegetation fraction)
	5	on (use maximum vegetation fraction)
	6	on (use VegFrac = VegFracGreen from input)
	7	off (use input LeafAreaIndex; use VegFrac = VegFracGreen from input)
	8	off (use input LeafAreaIndex; calculate VegFrac)
	9	off (use input LeafAreaIndex; use maximum vegetation fraction)
OptRainSnowPartition options for partitioning precipitation into rainfall & snowfall	1*	Jordan (1991) scheme
	2	BATS: when TemperatureAirRefHeight < freezing point+2.2 (Yang and Dickinson, 1996)
	3	TemperatureAirRefHeight < freezing point (Niu et al., 2011)
	4	Use WRF microphysics output (Barlage et al., 2015)
	5	Use wet-bulb temperature (Wang et al., 2019)
OptSoilWaterTranspiration options for soil moisture factor for stomatal resistance & ET	1*	Noah (soil moisture) (Ek et al., 2003)
	2	CLM (matric potential) (Oleson et al., 2004)
	3	SSiB (matric potential) (Xue et al., 1991)
OptGroundResistanceEvap options for ground resistant to evaporation/sublimation	1*	Sakaguchi and Zeng (2009) scheme
	2	Sellers (1992) scheme
	3	adjusted Sellers (1992) for wet soil
	4	Sakaguchi and Zeng (2009) for non-snow; rsurf = rsurf_snow for snow (set in NoahmpTable.TBL)
OptSurfaceDrag options for surface layer drag/exchange coefficient	1*	Monin-Obukhov (M-O) Similarity Theory (Brutsaert, 1982)
	2	original Noah (Chen et al. 1997)



OptStomataResistance	1*	Ball-Berry scheme (Ball et al., 1987; Bonan, 1996)
options for canopy stomatal resistance	2	Jarvis scheme (Jarvis, 1976)
OptSnowAlbedo	1*	BATS snow albedo (Dickinson et al., 1993)
options for ground snow surface albedo	2	CLASS snow albedo (Verseghy, 1991)
OptCanopyRadiationTransfer	1	modified two-stream (gap = f (solar angle, 3D structure, etc) < 1-VegFrac) (Niu and Yang, 2004)
options for canopy radiation transfer	2	two-stream applied to grid-cell (gap=0) (Niu et al., 2011)
	3*	two-stream applied to vegetated fraction (gap=1-VegFrac) (Dickinson, 1983; Sellers, 1985)
OptSnowSoilTempTime	1*	semi-implicit; flux top boundary condition (Niu et al., 2011)
options for snow/soil temperature time scheme (only layer 1)	2	full implicit (original Noah); temperature top boundary condition (Ek et al., 2003)
	3	same as 1, but snow cover for skin temperature calculation (Niu et al., 2011)
OptSnowThermConduct	1*	Stieglitz scheme (Yen, 1965)
options for snow thermal conductivity	2	Anderson (1976) scheme
	3	Constant (Niu et al., 2011)
	4	Verseghy (1991) scheme
	5	Douville scheme (Yen, 1981)
OptSoilTemperatureBottom	1	zero heat flux from bottom (DepthSoilTempBottom & TemperatureSoilBottom not used) (Niu et al., 2011)
options for lower boundary condition of soil temperature	2*	TemperatureSoilBottom at DepthSoilTempBottom (8m) read from a file (original Noah) (Ek et al., 2003)
OptSoilSupercoolWater	1*	No iteration (Niu and Yang, 2006)
options for soil supercooled liquid water	2	Koren's iteration (Koren et al., 1999)
OptRunoffSurface	1	TOPMODEL with groundwater (Niu et al., 2007)
options for surface runoff	2	TOPMODEL with an equilibrium water table (Niu et al., 2005)
	3*	Schaake scheme (original Noah) (Schaake et al., 1996)
	4	BATS surface and subsurface runoff (Yang and Dickinson, 1996)
	5	Miguez-Macho & Fan (MMF) groundwater scheme (Fan et al., 2007; Miguez-Macho et al. 2007)
	6	Variable Infiltration Capacity Model surface runoff scheme (Liang et al., 1994)
	7	Xinjiang Infiltration and surface runoff scheme (Jayawardena and Zhou, 2000)
	8	Dynamic VIC surface runoff scheme (Liang and Xie, 2003)



OptRunoffSubsurface options for drainage & subsurface runoff	1~8	similar to runoff option, separated from original Noah-MP runoff option, currently tested & recommended the same option# as surface runoff (default)
OptSoilPermeabilityFrozen options for frozen soil permeability	1*	linear effects, more permeable (Niu and Yang, 2006)
	2	nonlinear effects, less permeable (Koren et al., 1999)
OptDynVicInfiltration options for infiltration in dynamic VIC runoff scheme	1*	Philip scheme (Liang and Xie, 2003)
	2	Green-Ampt scheme (Liang and Xie, 2003)
	3	Smith-Parlange scheme (Liang and Xie, 2003)
OptTileDrainage options for tile drainage currently only tested & calibrated to work with runoff option=3	0*	No tile drainage
	1	on (simple scheme) (Valayamkunnath et al., 2022)
	2	on (Hooghoudt's scheme) (Valayamkunnath et al., 2022)
OptIrrigation options for irrigation	0*	No irrigation
	1	Irrigation on (Valayamkunnath et al., 2021)
	2	irrigation trigger based on crop season planting and harvesting dates (Valayamkunnath et al., 2021)
	3	irrigation trigger based on LeafAreaIndex threshold (Valayamkunnath et al., 2021)
OptIrrigationMethod options for irrigation method, only works when OptIrrigation > 0	0*	method based on geo_em fractions
	1	sprinkler method (Valayamkunnath et al., 2021)
	2	micro/drip irrigation (Valayamkunnath et al., 2021)
	3	surface flooding (Valayamkunnath et al., 2021)
OptCropModel options for crop model	0*	No crop model
	1	Liu, et al. (2016) crop scheme
OptSoilProperty options for defining soil properties	1*	use input dominant soil texture
	2	use input soil texture that varies with depth
	3	use soil composition (sand, clay, orgm) and pedotransfer function
	4	use input soil properties
OptPedotransfer options for pedotransfer functions, only works when OptSoilProperty=3	1*	Saxton and Rawls (2006) scheme
OptGlacierTreatment options for glacier treatment	1*	include phase change of glacier ice
	2	Glacier ice treatment more like original Noah

293

294

295

296

297

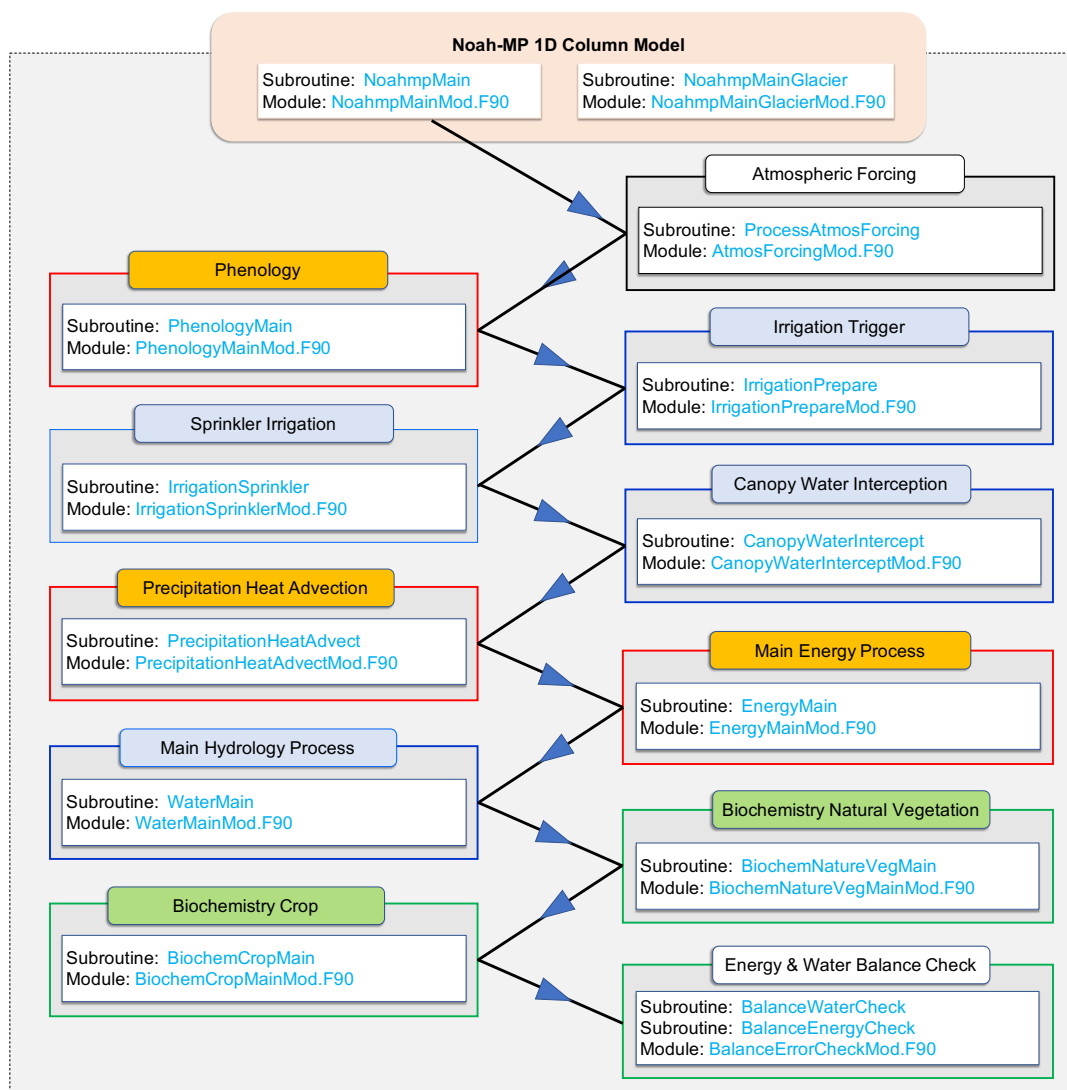
298

3. Enhanced model modularization in Noah-MP version 5.0

In the Noah-MP v5.0, we have modularized all model physics by separating and re-organizing each code subroutine into individual process-level Fortran module file with new descriptive, self-

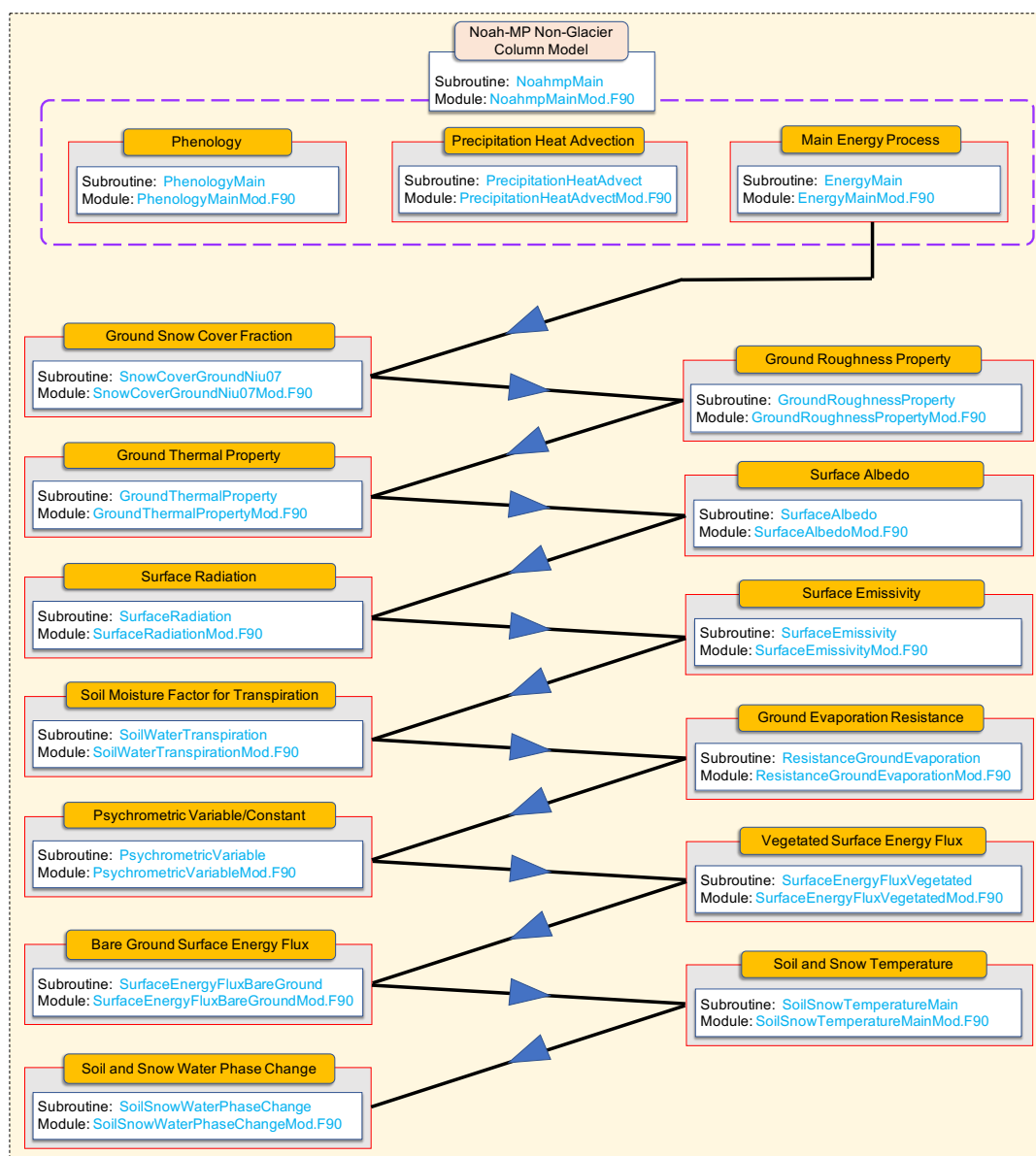


299 explanatory module and subroutine names. As such, each model physics or scheme has its own
300 separate module. Figure 4 shows the calling tree of the modularized Noah-MP main model physics
301 workflow. Figures 5-7 show the calling tree of the modularized energy, water, and carbon
302 processes, respectively. Compared to the previous Noah-MP versions that have a single lengthy
303 source file lumping together all model subroutines with non-self-explanatory names, the highly-
304 modularized model structure of the Noah-MP v5.0 provides a much more clear, neat, and
305 organized way for users and developers to understand and follow the model logics and physics.
306 These new modules use consistent coding format and standards, offering convenience for code
307 reading, writing, and debugging. The highly-modularized model structure also allows external
308 community weather/climate/hydrology models to easily adopt specific Noah-MP physical
309 processes/schemes as independent process-level module files and implement them for testing and
310 coupling.
311



312
313
314
315
316
317
318

Figure 4. The modularized Noah-MP main physics calling tree in version 5.0. Blue boxes indicate water processes, orange boxes indicate energy processes, and green boxes indicate biochemical processes. The direction of arrows indicates processes calling sequence and information flow. Note that the 1-D glacier column model has similar structures as the main non-glacier model, except that the vegetation-related processes are removed and soil is replaced by glacier ice.



319

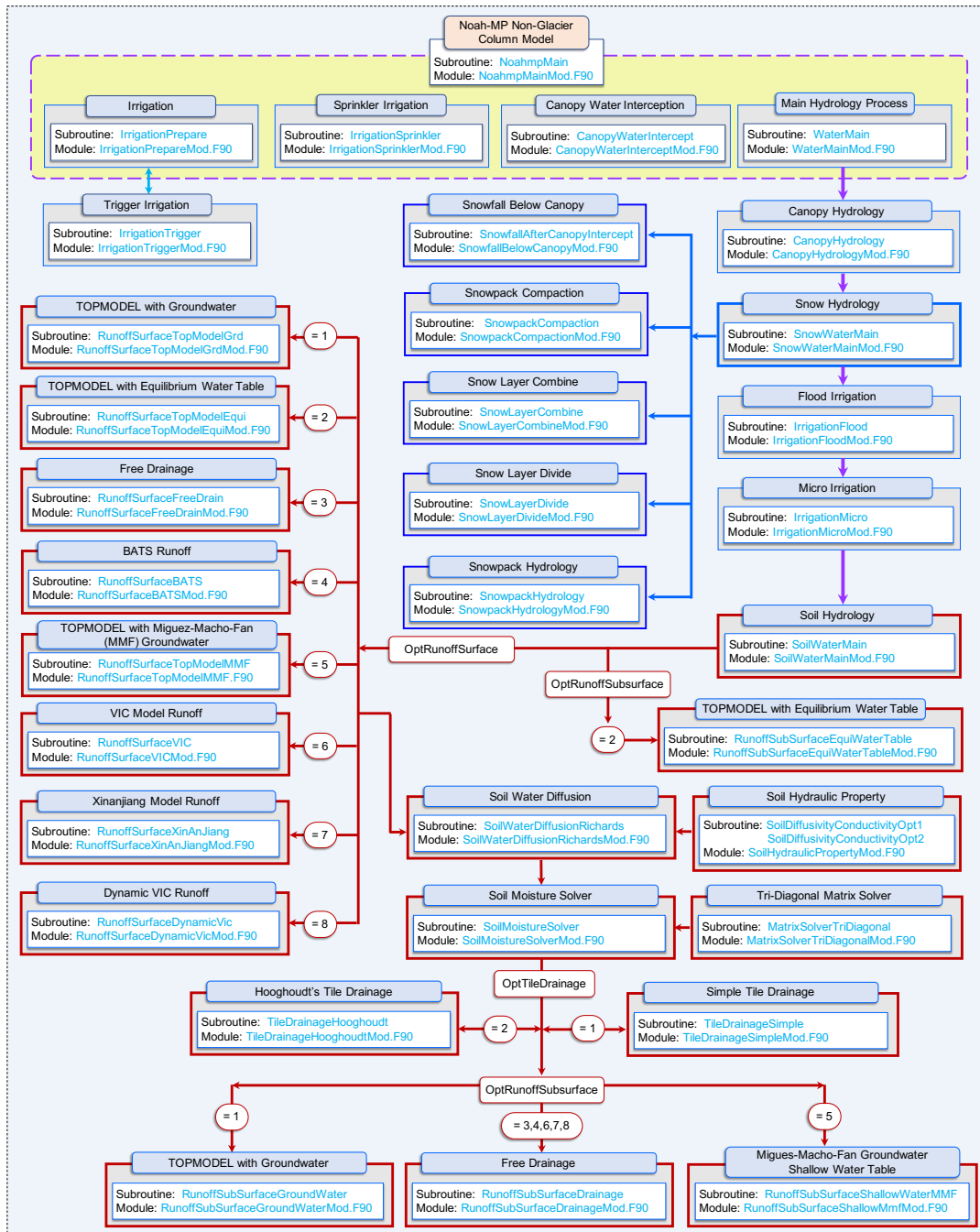
320

321

322

323

Figure 5. The modularized Noah-MP energy processes calling tree in version 5.0. Note that the glacier model has similar structures except that the vegetation-related processes are removed and soil is replaced by glacier ice.

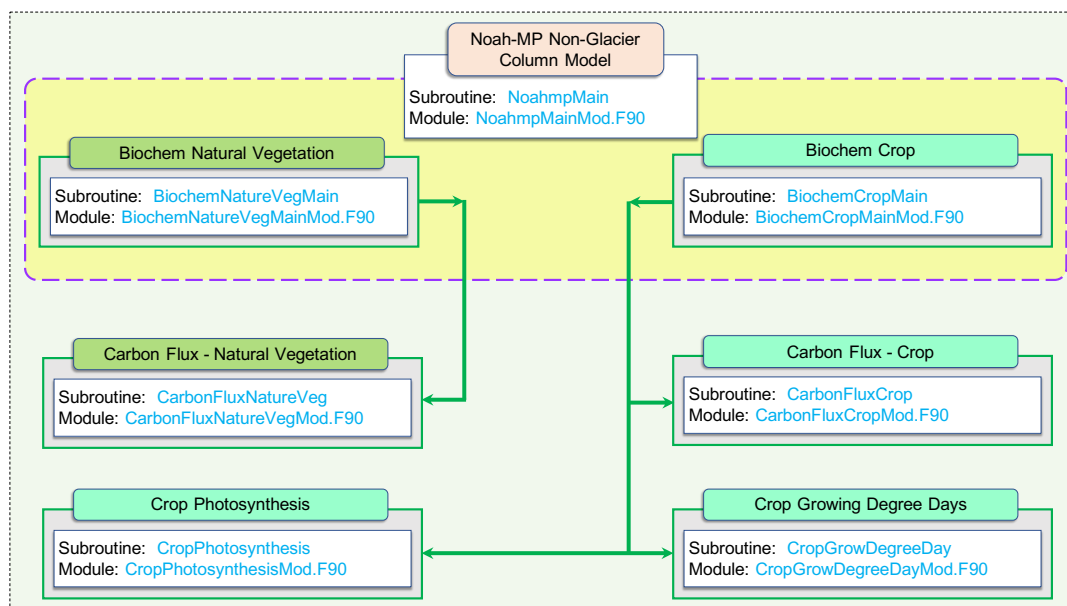


324
 325
 326
 327

Figure 6. The modularized Noah-MP water processes calling tree in version 5.0. Note that the glacier model has similar structures except that it only includes the snowpack processes and soil is replaced by glacier ice.



328



329

330 **Figure 7.** The modularized Noah-MP biochemical processes calling tree in version 5.0. Note that
 331 currently the Noah-MP v5.0 only includes carbon processes. Note that the CropPhotosynthesis
 332 module is not used currently to avoid inconsistency with the photosynthesis calculations from the
 333 canopy stomatal resistance module.

334

335

336 **4. Enhanced data structure in Noah-MP version 5.0**

337

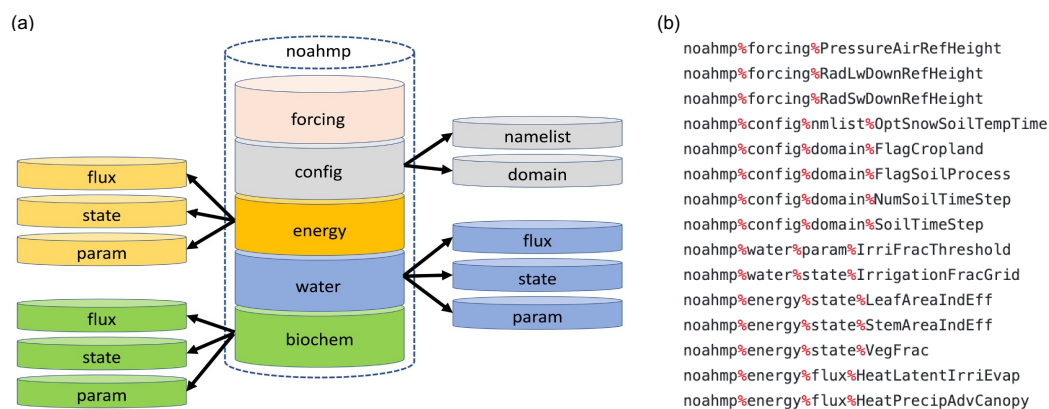
338 In the Noah-MP v5.0, we have enhanced data structure with new hierarchical data types, which
 339 allows a more efficient and convenient control of model variables and substantially simplifies code
 340 structures and calling interface (Section 5). Figure 8 summarizes the new Noah-MP data type
 341 hierarchy and gives some examples of model variable expression based on the hierarchical data
 342 types. Specifically, we have defined an overarching “noahmp” main data type, which includes
 343 “forcing” for atmospheric forcing variable type, “config” for model configuration variable type
 344 with “domain” and “namelist” subtypes, “energy” for energy-related variable type, “water” for
 345 water-related variable type, and “biochem” for biochemistry-related variable type. The “energy”,
 346 “water”, and “biochem” types are further divided into “flux”, “state”, and “param” subtypes for
 347 flux, state, and parameter variables. This hierarchical data structure provides a better organization
 348 and management of model variables and their physical attributes. We have also optimized the
 349 variable declaration and initialization structures based on those new data types and consistent
 350 coding format and standard. In addition, we have re-defined many key local model state, flux, and
 351 parameter variables in the base code to be global variables in the refactored code, which allows a



352 better track and management of these variables for diagnosis, transfer between Noah-MP and host
 353 models, and coupling with data assimilation systems.

354

355



356

357 **Figure 8.** (a) The new hierarchical “noahmp” data types in the Noah-MP version 5.0. (b) Examples
 358 of model variable expression using the hierarchical data types.

359

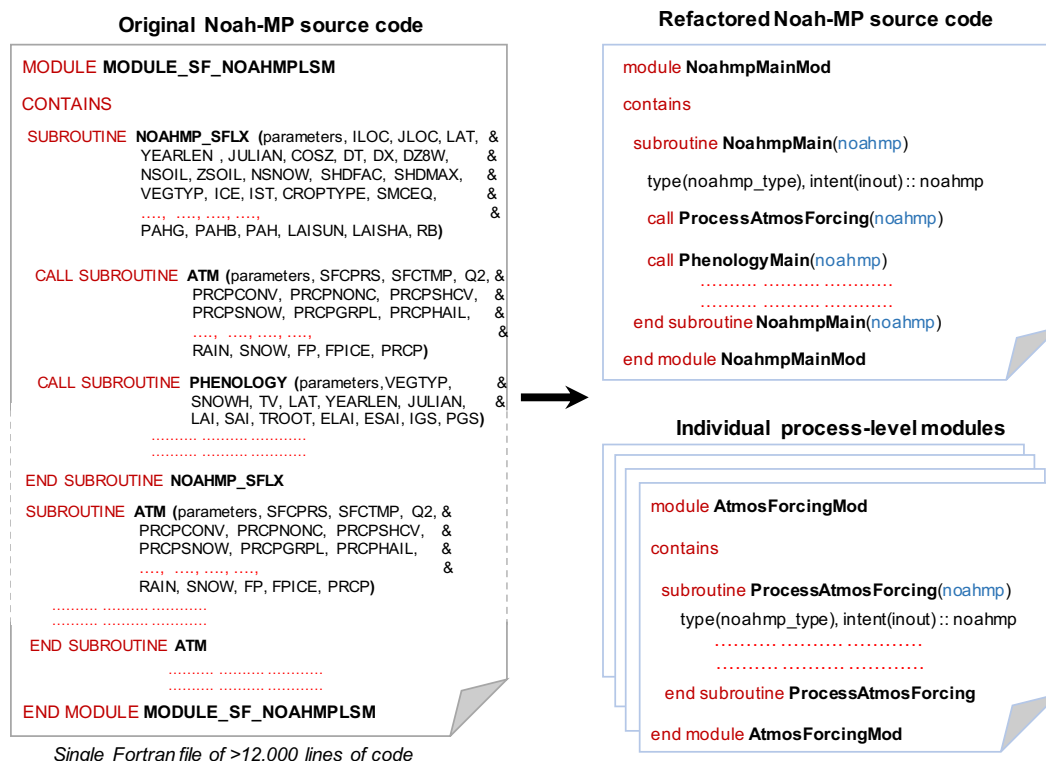
360

361 5. Enhanced code structure in Noah-MP version 5.0

362

363 Leveraging the model modularization (Section 3) and new data types (Section 4) in the Noah-MP
 364 v5.0, we have further refined the code structure and subroutine interface. A graphical
 365 representation of the refactored Noah-MP subroutine interface is depicted in Figure 9. Specifically,
 366 the refined subroutine interface only requires passing the “noahmp” data type instead of each
 367 individual variable names, because all relevant variables are defined and included in the “noahmp”
 368 data type. This significantly simplifies the code structure with much more concise and neat
 369 subroutine calls. The refined subroutine interface also makes future model development and code
 370 changes simpler, more efficient, and less error-prone. For instance, if users want to add/remove a
 371 variable for a specific physical scheme, they only need to edit as few as 3 module files: variable
 372 type definition module, variable initialization module, the target physical scheme module, and if
 373 needed, the variable input/output module. There is no need to go through and change all the
 374 subroutine calls and interfaces that use the target variable.

375



376

377

Figure 9. Demonstration of refactored subroutine interface and code structure in the Noah-MP version 5.0.

378

379

380

381

6. Enhanced variable naming in Noah-MP version 5.0

382

383

384

385

386

387

388

389

390

391

392

393

394

395

In the Noah-MP v5.0, we have also renamed all the model variables using a more descriptive and self-explanatory naming standard, which clarifies the physical meaning of variables directly by their names and hence substantially lowers the hurdles of reading and understanding the code and model physics. The original variable names in the previous Noah-MP versions are hard to understand, in which case users have to check back and forth the variable definition to know their physical meaning. For instance, the original variable name for canopy intercepted total water is “CMC”, while the new name is “CanopyTotalWater”. Table 2 gives more examples of the enhanced variable naming in Noah-MP v5.0. A detailed Noah-MP variable glossary listing variables’ original and new names, physical meaning, data type, and unit is provided in the technical documentation (He et al., 2023) and the community Noah-MP GitHub repository.



396 **Table 2.** Examples of new variable names based on a more descriptive and self-explanatory
 397 naming standard in the Noah-MP version 5.0, compared with the original names.

Variable physical meaning/definition	New name	Original name	Variable Type	Unit
wetted or snowed fraction of canopy	CanopyWetFrac	FWET	Real	-
canopy intercepted liquid water	CanopyLiqWater	CANLIQ	Real	mm
canopy intercepted ice	CanopyIce	CANICE	Real	mm
canopy intercepted total water	CanopyTotalWater	CMC	Real	mm
canopy capacity for snow interception	CanopyIceMax	MAXSNO	Real	mm
canopy capacity for liquid water interception	CanopyLiqWaterMax	MAXLIQ	Real	mm
ice fraction in snow layers	SnowIceFrac	FICE_SNOW	Real	-
bulk density of snowfall	SnowfallDensity	BDFALL	Real	kg/m ³
snow cover fraction	SnowCoverFrac	FSNO	Real	-
snow layer ice	SnowIce	SNICE	Real	mm
snow layer liquid water	SnowLiqWater	SNLIQ	Real	mm

398

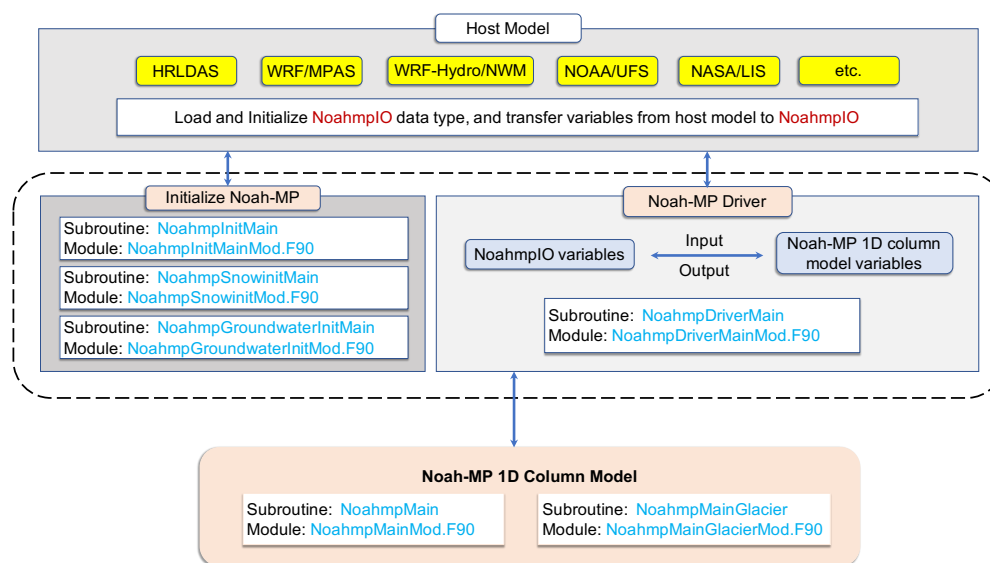
399

400 **7. Enhanced coupling structure with host models in Noah-MP version 5.0**

401

402 We have further updated the Noah-MP driver and interface coupled with potential host
 403 weather/climate/hydrology models. Figure 10 summarizes the interface and coupling structures in
 404 the Noah-MP v5.0. Specifically, the coupling interface includes: (1) defining a 2-D (for structured
 405 grid mesh) or vectorized (for unstructured grid mesh) Noah-MP input/output data type
 406 “NoahmpIO” to facilitate the input/output communication between host models and the core
 407 Noah-MP 1-D column model (“noahmp” data type); (2) the initialization of the “NoahmpIO”
 408 variables with values from host models; (3) the main Noah-MP driver that calls the core 1-D
 409 column model and transfers between the “NoahmpIO” and “noahmp” variables as part of
 410 input/output processes. Currently, the coupling of the Noah-MP v5.0 with the NCAR/HRLDAS
 411 system has been successfully completed. The coupling of Noah-MP v5.0 with the NASA/LIS
 412 system and the WRF-Hydro/NWM system is on-going. We also plan to couple the Noah-MP v5.0
 413 with other host models in the future (Section 9), such as WRF, MPAS, and NOAA/UFS. Because
 414 of the enhanced coupling interface and structure in Noah-MP v5.0, we will only need to slightly
 415 adapt the coupling interface and driver to allow it to work with different host models. We will
 416 manage and maintain the interface and driver code for each host model in the community Noah-
 417 MP GitHub repository to ensure the compatibility between host models and updated core Noah-
 418 MP source code in the future, which will allow smooth transition and seamless synthesizing of
 419 Noah-MP updates in host models.

420



421

422 **Figure 10.** Workflow of the Noah-MP v5.0 driver and interface structures to couple with various
 423 host weather/climate/hydrology models.

424

425

426 **8. Benchmarking for Noah-MP version 5.0**

427

428 To benchmark the functionality, reproducibility, and computational efficiency of the modernized
 429 Noah-MP code, we have conducted a series of hierarchical test simulations during the course of
 430 Noah-MP refactoring. Specifically, after refactoring each major Noah-MP model
 431 component/physics (e.g., water, energy, carbon, etc.) listed in Figure 4, we built simple driver
 432 modules to conduct benchmark simulations using each of these model component/physics to test
 433 and ensure the bit-for-bit consistency between the refactored code and base code for all Noah-MP
 434 physics options. Here is an example for the refactored Noah-MP water component model we built
 435 for benchmarking during the course of refactoring:
 436 https://github.com/cenlinhe/NoahMP_refactor/tree/water_refactor, which was used to test the bit-
 437 for-bit consistency between the refactored and base Noah-MP water component codes.

438

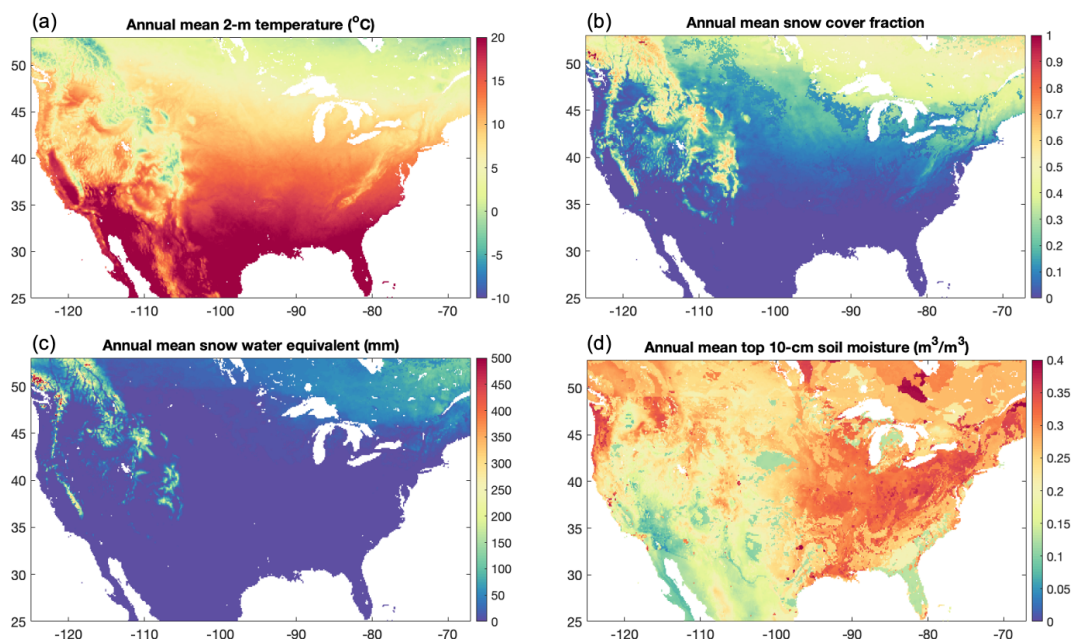
439 After we completed the entire model refactoring, we have conducted another set of test simulations
 440 using the completed Noah-MP v5.0 to ensure its bit-for-bit consistency with the base model code
 441 for all different combinations of physics options as well as to benchmark its computational
 442 efficiency. These tests were conducted via 1-year point-scale SNOTEL 804-site simulations, 1-
 443 year 12-km gridded continental US simulations, and 1-year 1-km gridded simulations over central
 444 US agricultural regions (particularly to test individual and combination of physics options related
 445 to crop, irrigation, tile drainage, and groundwater). The tests all showed exactly the same results
 446 between the refactored and base simulations, with similar computational efficiency.



447

448 In addition, in order to provide the community with reference Noah-MP v5.0 model datasets for
 449 future comparison and assessment, we have conducted 3 sets of benchmark simulations, including
 450 21-year (2000-2020) 12-km continental US simulations driven by the NLDAS-2 atmospheric
 451 forcings (Xia et al., 2012), 10-year (2009-2018) point-scale SNOTEL 804-site simulations over
 452 the western US driven by observed precipitation and temperature as well as other NLDAS-2
 453 atmospheric forcings downscaled to 90-m spatial resolution (He et al., 2021), and 1-year (2000)
 454 4-km dynamic crop simulations over the U.S. Corn Belt region driven by the convection-
 455 permitting WRF modeling (Zhang et al., 2020). We have archived all the atmospheric forcing
 456 datasets, model setup input datasets, and model output datasets for these benchmark simulations.
 457 Figure 11 shows an example of the model output. Note that a comprehensive evaluation of the
 458 simulation results is outside the scope of this model description paper and will be done in the next
 459 step.

460



461

462 **Figure 11.** Demonstration of 20-year (2001-2020) annual mean (a) 2-m temperature, (b) snow
 463 cover fraction, (c) snow water equivalent, and (d) top 10-cm soil moisture from the Noah-MP
 464 version 5.0 12-km continental US benchmark simulations driven by the NLDAS-2 atmospheric
 465 forcings.

466

467 **9. Model code and technical documentation for Noah-MP version 5.0**

468

469 We archive, manage, and maintain the Noah-MP v5.0 (together with previous code versions) at
 470 the NCAR community Noah-MP GitHub repository (<https://github.com/NCAR/noahmp>) for



471 public access. We have also created a comprehensive technical documentation (He et al., 2023)
472 for the Noah-MP v5.0, available at <http://dx.doi.org/10.5065/ew8g-yr95>, which provides detailed
473 descriptions of model physics and formulations.

474

475 **10. Conclusions and future plans**

476

477 In this study, we modernized the widely-used state-of-the-art Noah-MP LSM by adopting modern
478 Fortran code and data structures and standards, which substantially enhances the model modularity,
479 interoperability, and applicability. The modernized Noah-MP has been released as the model
480 version 5.0, which includes the following key features: (1) enhanced modularization and
481 interoperability by re-organizing model physics into individual process-level Fortran module files,
482 (2) enhanced data structure with new hierarchical data types and optimized variable declaration
483 and initialization structures, (3) enhanced code structure and calling workflow by leveraging the
484 new data structure and modularization, (4) enhanced (descriptive and self-explanatory) model
485 variable naming standard, and (5) enhanced driver and interface structure to couple with host
486 weather/climate/hydrology models. The base code used for modernization is the Noah-MP version
487 4.5 (released in December 2022), and the modernization effort does not change model physics. In
488 addition, we have created a comprehensive technical documentation (He et al., 2023) of the Noah-
489 MP v5.0, and a set of benchmark simulation datasets. The Noah-MP v5.0 has been coupled to the
490 NCAR/HRLDAS system. Currently, the work of coupling the Noah-MP v5.0 with the latest
491 NASA/LIS system and the WRF-Hydro/NWM system is on-going. In the future, we also plan to
492 couple the Noah-MP v5.0 to other weather and climate models, including WRF, MPAS, and
493 NOAA/UFS. Overall, the modernized open-source community Noah-MP model will allow a more
494 efficient and convenient process for future model developments and applications.

495

496

497 **Code and data availability**

498 The Noah-MP model code is available at <https://github.com/NCAR/noahmp>

499 The coupled HRLDAS/Noah-MP model code is available at <https://github.com/NCAR/hrlldas>

500 The Noah-MP technical documentation is available at <http://dx.doi.org/10.5065/ew8g-yr95>

501 The benchmark datasets can be provided by the corresponding author upon request, due to the
502 extremely large data size (8.8 TB).

503

504

505 **Author contribution**

506 CH, PV, and MB led the code refactoring effort with the help from all the other coauthors (FC,
507 DG, RC, GN, ZY, DN, ME, TS, RR). CH and PV led the technical documentation writing effort
508 with the help from all the other coauthors (MB, FC, DG, RC, GN, ZY, DN, ME, TS, RR). CH
509 conducted the benchmark model simulations. CH drafted the manuscript with improvements from
510 all the other coauthors (PV, FC, MB, DG, RC, GN, ZY, DN, ME, TS, RR).



511

512

513 **Competing interests**

514 The authors declare that they have no conflict of interest.

515

516

517 **Acknowledgements**

518 We thank Zhe Zhang (NCAR) and Ronnie Abolafia-Rosenzweig (NCAR) for helping with model
519 code testing and for helpful discussions. We also acknowledge the strong support from the entire
520 Noah-MP community. This study was supported by the US Geological Survey (USGS) Water
521 Mission Area's Integrated Water Prediction Program, NOAA's Climate Program Office's
522 Modeling, Analysis, Predictions, and Projections Program (MAPP), and the NCAR Water System
523 Program. National Center for Atmospheric Research (NCAR) is a major facility sponsored by the
524 National Science Foundation (NSF) under Cooperative Agreement #1852977. Any opinions,
525 findings, conclusions, or recommendations expressed in this publication are those of the authors
526 and do not necessarily reflect the views of the National Science Foundation.

527

528

529 **References**

- 530 Abolafia-Rosenzweig, R., He, C., Burns, S.P., Chen, F., 2021. Implementation and Evaluation of
531 a Unified Turbulence Parameterization Throughout the Canopy and Roughness Sublayer in
532 Noah-MP Snow Simulations. *J Adv Model Earth Syst* 13.
533 <https://doi.org/10.1029/2021MS002665>
- 534 Abolafia-Rosenzweig, R., He, C., Chen, F., 2022a. Winter and spring climate explains a large
535 portion of interannual variability and trend in western U.S. summer fire burned area. *Environ.*
536 *Res. Lett.* 17, 054030. <https://doi.org/10.1088/1748-9326/ac6886>
- 537 Abolafia-Rosenzweig, R., He, C., McKenzie Skiles, S., Chen, F., Gochis, D., 2022b. Evaluation
538 and Optimization of Snow Albedo Scheme in Noah-MP Land Surface Model Using In Situ
539 Spectral Observations in the Colorado Rockies. *J Adv Model Earth Syst* 14.
540 <https://doi.org/10.1029/2022MS003141>
- 541 Abolafia-Rosenzweig, R., He, C., Chen, F. et al. 2023a. High Resolution Forecasting of Summer
542 Drought in the Western United States. *Water Resources Research*, in review
- 543 Abolafia-Rosenzweig, R., He, C., Chen, F. et al. 2023b. Evaluating Noah-MP simulated post-fire
544 runoff and snowpack in Pacific-Northwest: challenges and future improvements, *Water*
545 *Resources Research*, in review
- 546 Anderson, E. A. (1976), A point energy and mass balance model of a snow cover, NOAA Tech.
547 Rep. NWS 19, 150 pp., Off. of Hydrol., Natl. Weather Serv., Silver Spring, Md.
- 548 Arsenault, K. R., Shukla, S., Hazra, A., Getirana, A., McNally, A., Kumar, S. V., ... & Verdin, J.
549 P. (2020). Better Advance Warnings of Drought. *Bulletin of the American Meteorological*
550 *Society*, 101(10), 899-903.



- 551 Ball, J. T., I. E. Woodrow, and J. A. Berry (1987), A model predicting sto- matal conductance and
552 its contribution to the control of photosynthesis under different environmental conditions, in
553 Process in Photosynthesis Research, vol. 1, edited by J. Biggins, pp. 221–234, Martinus Nijhoff,
554 Dordrecht, Netherlands.
- 555 Barlage, M., Tewari, M., Chen, F., Miguez-Macho, G., Yang, Z. L., & Niu, G. Y. (2015). The
556 effect of groundwater interaction in North American regional climate simulations with
557 WRF/Noah-MP. *Climatic Change*, 129, 485-498.
- 558 Barlage, M., Chen, F., Rasmussen, R., Zhang, Z., & Miguez-Macho, G. (2021). The importance
559 of scale-dependent groundwater processes in land-atmosphere interactions over the central
560 United States. *Geophysical Research Letters*, 48(5), e2020GL092171.
- 561 Blyth, E. M., Arora, V. K., Clark, D. B., Dadson, S. J., De Kauwe, M. G., Lawrence, D. M., ... &
562 Yuan, H. (2021). Advances in land surface modelling. *Current Climate Change Reports*, 7(2),
563 45-71.
- 564 Bonan, G. B. (1996), A land surface model (LSM version 1.0) for ecolog- ical, hydrological, and
565 atmospheric studies: Technical description and user’s guide, NCAR Tech. Note NCAR/TN-
566 417+STR, 150 pp., Natl. Cent. for Atmos. Res., Boulder, Colo.
- 567 Bonan, G. B., & Doney, S. C. (2018). Climate, ecosystems, and planetary futures: The challenge
568 to predict life in Earth system models. *Science*, 359(6375), eaam8328.
569 <https://doi.org/10.1126/science.aam8328>
- 570 Brunsell, N. A., de Oliveira, G., Barlage, M., Shimabukuro, Y., Moraes, E., & Aragao, L. (2021).
571 Examination of seasonal water and carbon dynamics in eastern Amazonia: a comparison of
572 Noah-MP and MODIS. *Theoretical and Applied Climatology*, 143, 571-586.
- 573 Brutsaert, W. A. (1982), *Evaporation Into the Atmosphere*, 299 pp., D. Reidel, Dordrecht,
574 Netherlands.
- 575 Cai, X., Yang, Z. L., David, C. H., Niu, G. Y., & Rodell, M. (2014). Hydrological evaluation of
576 the Noah-MP land surface model for the Mississippi River Basin. *Journal of Geophysical
577 Research: Atmospheres*, 119(1), 23-38.
- 578 Cai, X., Yang, Z. L., Fisher, J. B., Zhang, X., Barlage, M., & Chen, F. (2016). Integration of
579 nitrogen dynamics into the Noah-MP land surface model v1. 1 for climate and environmental
580 predictions. *Geoscientific Model Development*, 9(1), 1-15.
- 581 Chang, M., Cao, J., Zhang, Q., Chen, W., Wu, G., Wu, L., ... & Wang, X. (2022). Improvement of
582 stomatal resistance and photosynthesis mechanism of Noah-MP-WDDM (v1. 42) in simulation
583 of NO₂ dry deposition velocity in forests. *Geoscientific Model Development*, 15(2), 787-801.
- 584 Chen, F., & Dudhia, J. (2001). Coupling an advanced land surface–hydrology model with the Penn
585 State–NCAR MM5 Modeling System. Part I: Model implementation and sensitivity. *Monthly
586 Weather Review*, 129, 17. [https://doi.org/10.1175/1520-0493\(2001\)129<0569:caalsh>2.0.co;2](https://doi.org/10.1175/1520-0493(2001)129<0569:caalsh>2.0.co;2)
- 587 Chen, F., Janjić, Z., & Mitchell, K. (1997). Impact of atmospheric surface-layer parameterizations
588 in the new land-surface scheme of the NCEP Mesoscale Eta Model. *Boundary-Layer
589 Meteorology*, 85, 391–421. <https://doi.org/10.1023/A:1000531001463>



- 590 Chen, F., Mitchell, K., Schaake, J., Xue, Y., Pan, H.-L., Koren, V., et al. (1996). Modeling of land
591 surface evaporation by four schemes and comparison with FIFE observations. *Journal of*
592 *Geophysical Research: Atmospheres*, 101, 7251–7268. <https://doi.org/10.1029/95JD02165>
- 593 Chen, F., & Zhang, Y. (2009). On the coupling strength between the land surface and the
594 atmosphere: From viewpoint of surface exchange coefficients. *Geophysical Research*
595 *Letters*, 36(10).
- 596 Chen, L., Li, Y., Chen, F., Barr, A., Barlage, M., & Wan, B. (2016). The incorporation of an
597 organic soil layer in the Noah-MP land surface model and its evaluation over a boreal aspen
598 forest. *Atmospheric Chemistry and Physics*, 16(13), 8375-8387.
- 599 Dickinson, R. E. (1983), Land surface processes and climate-surface albedo and energy balance,
600 in *Theory of Climate*, *Adv. Geophys.*, vol. 25, edited by B. Saltzman, pp. 305–353, Academic,
601 San Diego, Calif.
- 602 Dickinson, R. E., A. Henderson-Sellers, and P. J. Kennedy (1993), Biosphere-Atmosphere
603 Transfer Scheme (BATS) version 1e as coupled to the NCAR Community Climate Model,
604 NCAR Tech. Note NCAR/TN- 387+STR, 80 pp., Natl. Cent. for Atmos. Res., Boulder, Colo.
- 605 Dickinson, R. E., M. Shaikh, R. Bryant, and L. Graumlich (1998), Interactive canopies for a
606 climate model, *J. Clim.*, 11, 2823–2836, doi:10.1175/1520-
607 0442(1998)011<2823:ICFACM>2.0.CO;2.
- 608 Ek, M. B., Mitchell, K. E., Lin, Y., Rogers, E., Grunmann, P., Koren, V., et al. (2003).
609 Implementation of Noah land surface model advances in the National Centers for
610 Environmental Prediction operational mesoscale Eta model. *Journal of Geophysical Research:*
611 *Atmospheres*, 108, 2002JD003296. <https://doi.org/10.1029/2002JD003296>
- 612 Fan, Y., Miguez-Macho, G., Weaver, C. P., Walko, R., & Robock, A. (2007). Incorporating water
613 table dynamics in climate modeling: 1. Water table observations and equilibrium water table
614 simulations. *Journal of Geophysical Research: Atmospheres*, 112(D10).
- 615 Gao, Y., Xiao, L., Chen, D., Chen, F., Xu, J., & Xu, Y. (2017). Quantification of the relative role
616 of land-surface processes and large-scale forcing in dynamic downscaling over the Tibetan
617 Plateau. *Climate Dynamics*, 48, 1705-1721.
- 618 Hazra, A., McNally, A., Slinski, K., Arsenault, K. R., Shukla, S., Getirana, A., ... & Koster, R. D.
619 (2023). NASA's NMME-based S2S hydrologic forecast system for food insecurity early
620 warning in southern Africa. *Journal of Hydrology*, 617, 129005.
- 621 He, C., F. Chen, M. Barlage, C. Liu, A. Newman, W. Tang, K. Ikeda, and R. Rasmussen (2019):
622 Can convection-permitting modeling provide decent precipitation for offline high-resolution
623 snowpack simulations over mountains, *J. Geophys. Res.-Atmos*,
624 124, <https://doi.org/10.1029/2019JD030823>
- 625 He, C., F. Chen, R. Abolafia-Rosenzweig, K. Ikeda, C. Liu, and R. Rasmussen (2021): What
626 causes the unobserved early-spring snowpack ablation in convection-permitting WRF modeling
627 over Utah mountains?, *J. Geophys. Res.-Atmos*, 126(22),
628 e2021JD035284, <https://doi.org/10.1029/2021JD035284>



- 629 He, C., P. Valayamkunnath, M. Barlage, F. Chen, D. Gochis, R. Cabell, T. Schneider, R.
630 Rasmussen, G.-Y. Niu, Z.-L. Yang, D. Niyogi, and M. Ek (2023): The Community Noah-MP
631 Land Surface Modeling System Technical Description Version 5.0. (*No. NCAR/TN-575+STR*),
632 <http://dx.doi.org/10.5065/ew8g-yr95>
- 633 Ingwersen, J., Högy, P., Wizemann, H. D., Warrach-Sagi, K., & Streck, T. (2018). Coupling the
634 land surface model Noah-MP with the generic crop growth model Gecros: Model description,
635 calibration and validation. *Agricultural and forest meteorology*, 262, 322-339.
- 636 Jarvis, P. G. (1976), The interpretation of the variations in leaf water poten- tial and stomatal
637 conductance found in canopies in the field, *Philos. Trans. R. Soc. B*, 273, 593–610,
638 doi:10.1098/rstb.1976.0035.
- 639 Jayawardena, A. W. and Zhou, M. C.: A modified spatial soil moisture storage capacity
640 distribution curve for the Xinanjiang model, *Journal of Hydrology*, 227, 93–113,
641 [https://doi.org/10.1016/S0022-1694\(99\)00173-0](https://doi.org/10.1016/S0022-1694(99)00173-0), 2000.
- 642 Jiang, Y., Chen, F., Gao, Y., He, C., Barlage, M., & Huang, W. (2020). Assessment of uncertainty
643 sources in snow cover simulation in the Tibetan Plateau. *Journal of Geophysical Research:*
644 *Atmospheres*, 125(18), e2020JD032674.
- 645 Jiang, Y., Gao, Y., He, C., Liu, B., Pan, Y., & Li, X. (2021). Spatiotemporal distribution and
646 variation of wind erosion over the Tibetan Plateau based on a coupled land-surface wind-
647 erosion model. *Aeolian Research*, 50, 100699.
- 648 Jordan, R. (1991), A one-dimensional temperature model for a snow cover, *Spec. Rep. 91–16*,
649 *Cold Reg. Res. and Eng. Lab., U.S. Army Corps of Eng., Hanover, N. H.*
- 650 Ju, C., Li, H., Li, M., Liu, Z., Ma, Y., Mamtimin, A., ... & Song, Y. (2022). Comparison of the
651 Forecast Performance of WRF Using Noah and Noah-MP Land Surface Schemes in Central
652 Asia Arid Region. *Atmosphere*, 13(6), 927.
- 653 Koren, V., J. C. Schaake, K. E. Mitchell, Q.-Y. Duan, F. Chen, and J. M. Baker (1999), A
654 parameterization of snowpack and frozen ground intended for NCEP weather and climate
655 models, *J. Geophys. Res.*, 104, 19,569–19,585, doi:10.1029/1999JD900232.
- 656 Kumar, S. V., Holmes, T., Andela, N., Dharssi, I., Hain, C., Peters-Lidard, C., ... & Getirana, A.
657 (2021). The 2019–2020 Australian drought and bushfires altered the partitioning of
658 hydrological fluxes. *Geophysical Research Letters*, 48(1), e2020GL091411.
- 659 Li, X., Wu, T., Zhu, X., Jiang, Y., Hu, G., Hao, J., ... & Ying, X. (2020). Improving the Noah-MP
660 model for simulating hydrothermal regime of the active layer in the permafrost regions of the
661 Qinghai-Tibet Plateau. *Journal of Geophysical Research: Atmospheres*, 125(16),
662 e2020JD032588.
- 663 Li, J., Chen, F., Lu, X., Gong, W., Zhang, G., & Gan, Y. (2020). Quantifying contributions of
664 uncertainties in physical parameterization schemes and model parameters to overall errors in
665 Noah-MP dynamic vegetation modeling. *Journal of Advances in Modeling Earth Systems*, 12.
666 <https://doi.org/10.1029/2019MS001914>
- 667 Li, L., Yang, Z. L., Matheny, A. M., Zheng, H., Swenson, S. C., Lawrence, D. M., ... & Leung, L.
668 R. (2021). Representation of plant hydraulics in the Noah-MP land surface model: Model



- 669 development and multiscale evaluation. *Journal of Advances in Modeling Earth Systems*, 13(4),
670 e2020MS002214.
- 671 Li, M., Wu, P., Ma, Z., Lv, M., Yang, Q., & Duan, Y. (2022). The decline in the groundwater table
672 depth over the past four decades in China simulated by the Noah-MP land model. *Journal of*
673 *Hydrology*, 607, 127551.
- 674 Liang, J., Yang, Z., & Lin, P. (2019). Systematic hydrological evaluation of the Noah-MP land
675 surface model over China. *Advances in Atmospheric Sciences*, 36, 1171-1187.
- 676 Liang, X., Lettenmaier, D. P., Wood, E. F., & Burges, S. J. (1994). A simple hydrologically based
677 model of land surface water and energy fluxes for general circulation models. *Journal of*
678 *Geophysical Research: Atmospheres*, 99(D7), 14415-14428.
- 679 Liang, X., & Xie, Z. (2003). Important factors in land-atmosphere interactions: surface runoff
680 generations and interactions between surface and groundwater. *Global and Planetary Change*,
681 38(1-2), 101-114.
- 682 Liu, X., Chen, F., Barlage, M., Zhou, G., & Niyogi, D. (2016). Noah-MP-Crop: Introducing
683 dynamic crop growth in the Noah-MP land surface model. *Journal of Geophysical Research:*
684 *Atmospheres*, 121(23), 13-953.
- 685 McDaniel, R., Liu, Y., Valayamkunnath, P., Barlage, M., Gochis, D., Cosgrove, B. A., & Flowers,
686 T. (2020, December). Moisture condition impact and seasonality of National Water Model
687 performance under different runoff-infiltration partitioning schemes. In *AGU Fall Meeting*
688 *Abstracts (Vol. 2020, pp. H111-0028)*.
- 689 Miguez-Macho, G., Fan, Y., Weaver, C. P., Walko, R., & Robock, A. (2007). Incorporating water
690 table dynamics in climate modeling: 2. Formulation, validation, and soil moisture
691 simulation. *Journal of Geophysical Research: Atmospheres*, 112(D13).
- 692 Nie, W., Kumar, S. V., Arsenault, K. R., Peters-Lidard, C. D., Mladenova, I. E., Bergaoui, K., ...
693 & Navari, M. (2022). Towards effective drought monitoring in the Middle East and North
694 Africa (MENA) region: implications from assimilating leaf area index and soil moisture into
695 the Noah-MP land surface model for Morocco. *Hydrology and Earth System Sciences*, 26(9),
696 2365-2386.
- 697 Niu, G.-Y., and Z.-L. Yang (2004), The effects of canopy processes on snow surface energy and
698 mass balances, *J. Geophys. Res.*, 109, D23111, doi:10.1029/2004JD004884.
- 699 Niu, G.-Y., Z.-L. Yang, R. E. Dickinson, and L. E. Gulden (2005), A simple TOPMODEL-based
700 runoff parameterization (SIMTOP) for use in global climate models, *J. Geophys. Res.*, 110,
701 D21106, doi:10.1029/2005JD006111.
- 702 Niu, G.-Y., and Z.-L. Yang (2006), Effects of frozen soil on snowmelt runoff and soil water
703 storage at a continental scale, *J. Hydrometeorol.*, 7, 937-952, doi:10.1175/JHM538.1.
- 704 Niu, G.-Y., Z.-L. Yang, R. E. Dickinson, L. E. Gulden, and H. Su (2007), Development of a simple
705 groundwater model for use in climate models and evaluation with Gravity Recovery and
706 Climate Experiment data, *J. Geophys. Res.*, 112, D07103, doi:10.1029/2006JD007522.
- 707 Niu, G.-Y., Yang, Z.-L., Mitchell, K. E., Chen, F., Ek, M. B., Barlage, M., et al. (2011). The
708 community Noah land surface model with multiparameterization options (Noah-MP): 1.



- 709 Model description and evaluation with local-scale measurements. *Journal of Geophysical*
710 *Research*, 116, D12109. <https://doi.org/10.1029/2010JD015139>
- 711 Niu, G. Y., Fang, Y. H., Chang, L. L., Jin, J., Yuan, H., & Zeng, X. (2020). Enhancing the Noah-
712 MP ecosystem response to droughts with an explicit representation of plant water storage
713 supplied by dynamic root water uptake. *Journal of Advances in Modeling Earth*
714 *Systems*, 12(11), e2020MS002062.
- 715 Oleson, K. W., et al. (2004), Technical description of the Community Land Model (CLM), NCAR
716 Tech. Note NCAR/TN-461+STR, 174 pp., Natl. Cent. for Atmos. Res., Boulder, Colo.
717 (Available at www.cgd.ucar.edu/tss/clm/distribution/clm3.0/index.html.)
- 718 Patel, P., Jamshidi, S., Nadimpalli, R., Aliaga, D. G., Mills, G., Chen, F., ... & Niyogi, D. (2022).
719 Modeling Large-Scale Heatwave by Incorporating Enhanced Urban Representation. *Journal of*
720 *Geophysical Research: Atmospheres*, 127(2), e2021JD035316.
- 721 Sakaguchi, K., & Zeng, X. (2009). Effects of soil wetness, plant litter, and under-canopy
722 atmospheric stability on ground evaporation in the Community Land Model (CLM3. 5). *Journal*
723 *of Geophysical Research: Atmospheres*, 114(D1).
- 724 Salamanca, F., Zhang, Y., Barlage, M., Chen, F., Mahalov, A., & Miao, S. (2018). Evaluation of
725 the WRF-urban modeling system coupled to Noah and Noah-MP land surface models over a
726 semiarid urban environment. *Journal of Geophysical Research: Atmospheres*, 123(5), 2387-
727 2408.
- 728 Saxton, K. E., & Rawls, W. J. (2006). Soil water characteristic estimates by texture and organic
729 matter for hydrologic solutions. *Soil science society of America Journal*, 70(5), 1569-1578.
- 730 Sellers, P. J. (1985), Canopy reflectance, photosynthesis and transpiration, *Int. J. Remote Sens.*, 6,
731 1335–1372, doi:10.1080/01431168508948283.
- 732 Sellers, P. J., M. D. Heiser, and F. G. Hall (1992), Relations between surface conductance and
733 spectral vegetation indices at intermediate (100 m² to 15 km²) length scales, *J. Geophys. Res.*,
734 97, 19,033–19,059, doi:10.1029/92JD01096.
- 735 Schaake, J. C., V. I. Koren, Q.-Y. Duan, K. E. Mitchell, and F. Chen (1996), Simple water balance
736 model for estimating runoff at different spatial and temporal scales, *J. Geophys. Res.*, 101,
737 7461–7475, doi:10.1029/95JD02892.
- 738 Suzuki, K., & Zupanski, M. (2018). Uncertainty in solid precipitation and snow depth prediction
739 for Siberia using the Noah and Noah-MP land surface models. *Frontiers of Earth Science*, 12,
740 672-682.
- 741 Valayamkunnath, P., Chen, F., Barlage, M. J., Gochis, D. J., Franz, K. J., & Cosgrove, B. A. (2021,
742 January). Impact of Agriculture Management Practices on the National Water Model Simulated
743 Streamflow. In 101st American Meteorological Society Annual Meeting. AMS.
- 744 Valayamkunnath, P., Gochis, D. J., Chen, F., Barlage, M., & Franz, K. J. (2022). Modeling the
745 hydrologic influence of subsurface tile drainage using the National Water Model. *Water*
746 *Resources Research*, 58(4), e2021WR031242.
- 747 Versegny, D. L. (1991), CLASS-A Canadian land surface scheme for GCMS: I. Soil model, *Int. J.*
748 *Climatol.*, 11, 111–133, doi:10.1002/joc.3370110202.



- 749 Wang, P., Niu, G. Y., Fang, Y. H., Wu, R. J., Yu, J. J., Yuan, G. F., ... & Scott, R. L. (2018).
750 Implementing dynamic root optimization in Noah-MP for simulating phreatophytic root water
751 uptake. *Water Resources Research*, 54(3), 1560-1575.
- 752 Wang, W., Yang, K., Zhao, L., Zheng, Z., Lu, H., Mamtimin, A., ... & Moore, J. C. (2020).
753 Characterizing surface albedo of shallow fresh snow and its importance for snow ablation on
754 the interior of the Tibetan Plateau. *Journal of Hydrometeorology*, 21(4), 815-827.
- 755 Wang, W., He, C., Moore, J., Wang, G., & Niu, G. Y. (2022). Physics-Based Narrowband Optical
756 Parameters for Snow Albedo Simulation in Climate Models. *Journal of Advances in Modeling
757 Earth Systems*, 14(1), e2020MS002431.
- 758 Wang, Y. H., Broxton, P., Fang, Y., Behrangi, A., Barlage, M., Zeng, X., & Niu, G. Y. (2019). A
759 wet-bulb temperature-based rain-snow partitioning scheme improves snowpack prediction over
760 the drier western United States. *Geophysical Research Letters*, 46(23), 13825-13835.
- 761 Warrach-Sagi, K., J. Ingwersen, T. Schwitalla, C. Troost, J. Aurbacher, L. Jach, T. Berger, T.
762 Streck, and V. Wulfmeyer, 2022: Noah-MP with the generic crop growth model Gecros in the
763 WRF model: Effects of dynamic crop growth on land-atmosphere interaction. *J Geophys Res-
764 Atmos*, 127(14), e2022JD036518. DOI:10.1029/2022JD036518
- 765 Wrzesien, M. L., Pavelsky, T. M., Kapnick, S. B., Durand, M. T., & Painter, T. H. (2015).
766 Evaluation of snow cover fraction for regional climate simulations in the Sierra N
767 evada. *International Journal of Climatology*, 35(9), 2472-2484.
- 768 Wu, W. Y., Yang, Z. L., & Barlage, M. (2021). The Impact of Noah-MP Physical
769 Parameterizations on Modeling Water Availability during Droughts in the Texas–Gulf
770 Region. *Journal of Hydrometeorology*, 22(5), 1221-1233.
- 771 Xia, Y., K. Mitchell, M. Ek, J. Sheffield, B. Cosgrove, E. Wood, L. Luo, C. Alonge, H. Wei, J.
772 Meng, B. Livneh, D. Lettenmaier, V. Koren, Q. Duan, K. Mo, Y. Fan, and D. Mocko (2012).
773 Continental-scale water and energy flux analysis and validation for the North American Land
774 Data Assimilation System project phase 2 (NLDAS-2): 1. Intercomparison and application of
775 model products. *J. Geophys. Res.*, 117, D03109, doi:10.1029/2011JD016048
- 776 Xu, T., Chen, F., He, X., Barlage, M., Zhang, Z., Liu, S., & He, X. (2021). Improve the
777 performance of the noah-MP-crop model by jointly assimilating soil moisture and vegetation
778 phenology data. *Journal of Advances in Modeling Earth Systems*, 13(7), e2020MS002394.
- 779 Xu, X., Chen, F., Shen, S., Miao, S., Barlage, M., Guo, W., & Mahalov, A. (2018). Using WRF-
780 urban to assess summertime air conditioning electric loads and their impacts on urban weather
781 in Beijing. *Journal of Geophysical Research: Atmospheres*, 123(5), 2475-2490.
- 782 Xue, Y., P. J. Sellers, J. L. Kinter, and J. Shukla (1991), A simplified bio- sphere model for global
783 climate studies, *J. Clim.*, 4, 345–364, doi:10.1175/1520-
784 0442(1991)004<0345:ASBMFG>2.0.CO;2.
- 785 Yang, Z.-L., and R. E. Dickinson (1996), Description of the Biosphere- Atmosphere Transfer
786 Scheme (BATS) for the soil moisture workshop and evaluation of its performance, *Global
787 Planet. Change*, 13, 117–134, doi:10.1016/0921-8181(95)00041-0.



- 788 Yang, Z. L., Niu, G. Y., Mitchell, K. E., Chen, F., Ek, M. B., Barlage, M., ... & Xia, Y. (2011).
789 The community Noah land surface model with multiparameterization options (Noah-MP): 2.
790 Evaluation over global river basins. *Journal of Geophysical Research: Atmospheres*, 116(D12).
791 Yen, Y. C. (1965). Effective thermal conductivity and water vapor diffusivity of naturally
792 compacted snow. *Journal of Geophysical Research*, 70(8), 1821-1825.
- 793 Yen, Y. C. (1981). Review of thermal properties of snow, ice, and sea ice (Vol. 81, No. 10). US
794 Army, Corps of Engineers, Cold Regions Research and Engineering Laboratory.
- 795 Zhang, G., Chen, F., & Gan, Y. (2016). Assessing uncertainties in the Noah-MP ensemble
796 simulations of a cropland site during the Tibet Joint International Cooperation program field
797 campaign. *Journal of Geophysical Research: Atmospheres*, 121, 9576–9596. <https://doi.org/10.1002/2016JD024928>
798
- 799 Zhang, X. Y., Jin, J., Zeng, X., Hawkins, C. P., Neto, A. A., & Niu, G. Y. (2022a). The
800 compensatory CO₂ fertilization and stomatal closure effects on runoff projection from 2016–
801 2099 in the western United States. *Water Resources Research*, 58(1), e2021WR030046.
- 802 Zhang, X., Xie, Z., Ma, Z., Barron-Gafford, G. A., Scott, R. L., & Niu, G. Y. (202b). A Microbial-
803 Explicit Soil Organic Carbon Decomposition Model (MESDM): Development and Testing at a
804 Semiarid Grassland Site. *Journal of Advances in Modeling Earth Systems*, 14(1),
805 e2021MS002485.
- 806 Zhang, Z., Barlage, M., Chen, F., Li, Y., Helgason, W., Xu, X., ... & Li, Z. (2020). Joint modeling
807 of crop and irrigation in the central United States using the Noah-MP land surface
808 model. *Journal of Advances in Modeling Earth Systems*, 12(7), e2020MS002159.
- 809 Zhang, Z., Chen, F., Barlage, M., Bortolotti, L. E., Famiglietti, J., Li, Z., ... & Li, Y. (2022).
810 Cooling Effects Revealed by Modeling of Wetlands and Land-Atmosphere Interactions. *Water*
811 *Resources Research*, 58(3), e2021WR030573.
- 812 Zhang, Z., Li, Y., Chen, F., Harder, P., Helgason, W., Famiglietti, J., Valayamkunnath, P., He, C.,
813 and Li, Z.: Developing Spring Wheat in the Noah-MP LSM (v4.4) for Growing Season
814 Dynamics and Responses to Temperature Stress, *Geosci. Model Dev. Discuss.* [preprint],
815 <https://doi.org/10.5194/gmd-2022-311>, in review, 2023.
- 816 Zhuo, L., Dai, Q., Han, D., Chen, N., & Zhao, B. (2019). Assessment of simulated soil moisture
817 from WRF Noah, Noah-MP, and CLM land surface schemes for landslide hazard
818 application. *Hydrology and Earth System Sciences*, 23(10), 4199-4218.
- 819 Zonato, A., Martilli, A., Gutierrez, E., Chen, F., He, C., Barlage, M., ... & Giovannini, L. (2021).
820 Exploring the effects of rooftop mitigation strategies on urban temperatures and energy
821 consumption. *Journal of Geophysical Research: Atmospheres*, 126(21), e2021JD035002.
822